The American Society of Mechanical Engineers

Reprinted From
MD-Vol. 43, Material Parameter Estimation for Modern Constitutive Equations
Editors: L. A. Bertram, S. B. Brown, and A. D. Freed
Book No. H00848 - 1993

VISCOPLASTIC MODEL DEVELOPMENT WITH AN EYE TOWARDS CHARACTERIZATION

Alan D. Freed
NASA Lewis Research Center
Cleveland, Ohio

Kevin P. Walker
Engineering Science Software, Inc.
Smithfield, Rhode Island

Abstract

A viscoplastic theory is developed that reduces analytically to creep theory under steady-state conditions. A viscoplastic model is constructed within this theoretical framework by defining material functions that have close ties to the physics of inelasticity. As a consequence, this model is easily characterized—only steady-state creep data, monotonic stress-strain curves, and saturated stress-strain hysteresis loops are required. The model is applied to the copper alloy NARloy Z.

1 Introduction

In mankind's enduring pursuit to go faster and further with greater economy and safety in its diverse variety of vehicles that travel across land and sea or through air and space, we are taxing our materials to their utmost capabilities. Consequently, the need for accurate material models to describe the various physical properties of a given material is much more critical in the design and development of these vehicles than it has ever been, and this need can only be expected to continue to grow.

The analysis of metallic response for high temperature applications requires mathematical models capable of predicting accurately the short-term plastic strains, the long-term creep strains, and interactions between them. Viscoplastic models attempt to do that. Multiaxial, cyclic and non-isothermal loading histories are normal service conditions, not exceptional ones, all of which challenge the predictive capabilities of such models.

Prior to the advent of the computer, viscoplasticity was a theory in its infancy; however, over the past two decades substantial advancements have been made to the theory. Because of viscoplasticity's innate nature, which leads to systems of first-order, ordinary, differential equations that are nonlinear, coupled and mathematically stiff, a unique mathematical structure (like that of elasticity) is not to be expected. Nevertheless, these past two decades have given the community a vast wealth of experience with a variety of evolution equations—what works, what does not, and in many cases, some physical insight as to why. Using this experience base, we have set out to develop a viscoplastic model whose predictive capabilities are in reasonable agreement with experiments. A special emphasis in this development process was that the resulting model must be characterized easily. The need to follow this requirement is vital. Experience has taught us that a model's ease of characterization without calibration via exotic experiments is often

considered by many industrial users of viscoplasticity to be of greater value than the model's ability to predict accurately a material's behavior (within reason). We therefore seek to strike a balance between accuracy and ease of characterization using physics as our guidepost.

The paper begins with a brief overview of the theories of elasticity and creep. This is followed by a definition of viscoplastic flow and the introduction of the required internal state variables. The next section demonstrates how a viscoplastic theory can be constructed to reduce analytically to creep theory under steady-state conditions. This important section demonstrates how a bridge between these two theories can be built—a concept that is not prevalent in the viscoplastic literature. By building this bridge, the model not only has a stronger physical base, but it also reduces substantially the complexity of material characterization. The section that follows describes how the various internal state variables are assumed to evolve, and the physical reasoning why they are so chosen. A succinct description of the viscoplastic model ensues, which is followed by a section on how we go about characterizing our viscoplastic model. For illustrative purposes, the copper alloy NARloy Z is modeled. This material finds applications where moderate strength is required under conditions of very high heat flux, *e.g.* it is used as the nozzle liner material in the main rocket engines of NASA's space shuttles where steep, rapidly applied, thermal gradients cause large localized strains.

2 Elasticity

The stress, σ_{ij}, is taken to be related to the infinitesimal strain, ϵ_{ij}, through the constitutive equations of an isotropic Hookean material, *viz.*

$$S_{ij} = 2\mu\big(E_{ij} - \varepsilon^p_{ij}\big) \qquad \text{where} \qquad \varepsilon^p_{kk} = 0\,, \tag{1}$$

and

$$\sigma_{kk} = 3\kappa\big(\epsilon_{kk} - \alpha(T - T_0)\delta_{kk}\big)\,, \tag{2}$$

which are characterized by the shear, μ, and bulk, κ, elastic moduli, and where

$$S_{ij} = \sigma_{ij} - {}^1\!/_3\,\sigma_{kk}\,\delta_{ij} \qquad \text{and} \qquad E_{ij} = \epsilon_{ij} - {}^1\!/_3\,\epsilon_{kk}\,\delta_{ij} \tag{3}$$

denote the deviatoric stress and strain, respectively. The mean coefficient of thermal expansion, α, acts on the difference between the current temperature, T, and some reference temperature, T_0. The Kronecker delta, δ_{ij}, has the value 1 if $i = j$, otherwise it is 0. Repeated Latin indices are summed from 1 to 3 in the usual manner. Equation (1) characterizes the deviatoric stress response, while Eqn. (2) characterizes the hydrostatic stress response. The plastic strain, ε^p_{ij}, and thermal strain, $\alpha(T - T_0)\delta_{ij}$, are, in essence, eigenstrains that represent deviations from deviatoric and hydrostatic elastic behaviors, respectively.

Young's modulus, E, and Poisson's ratio, ν, are the two elastic constants that are usually determined via experiment. The expressions,

$$\mu = \frac{E}{2(1+\nu)} \qquad \text{and} \qquad \kappa = \frac{E}{3(1-2\nu)}\,, \tag{4}$$

define their interdependence with the elastic moduli of Eqns (1) and (2). Only two elastic moduli are independent for elastically isotropic materials. Values for the elastic constants of NARloy Z (typical composition: Cu–3%Ag–0.5%Zr) are given in Table 1.

3 Creep

The evolution of plastic strain which describes the classical theory of creep (ODQVIST, 1974) is given by

$$\dot{\varepsilon}^p_{ij}\Big|_{\rm ss} = {}^1\!/_2\,\|\dot{\boldsymbol{\varepsilon}}^p\|_{\rm ss}\,\frac{S_{ij}}{\|\boldsymbol{S}\|}\,, \tag{5}$$

Constant	Units	Value
α	K^{-1}	16.5×10^{-6}
μ_0	MPa	52,000
μ_1	MPa/K	-14
ν	—	0.34
$\mu = \mu_0 + \mu_1 T$,		T is in K

Table 1: Elastic constants for NARloy Z (*Materials Properties Manual*, 1986).

with the subscript 'ss' implying steady state, and where $\|\dot{\boldsymbol{\varepsilon}}^p\|$ denotes the magnitude of plastic strain-rate and $\|\boldsymbol{S}\|$ denotes the magnitude of deviatoric stress. The subscript signifying steady state is not attached to S_{ij} because stress is a controllable external variable, whereas creep rate is a response variable. This equation states that an increment in creep strain accumulates in the current direction of the deviatoric stress. A dot is placed over a variable to signify its time rate-of-change.

The norms, or magnitudes, pertaining to the deviatoric tensors of this paper are defined by

$$\|\boldsymbol{I}\| = \sqrt{2\, I_{ij}\, I_{ij}} \qquad \text{and} \qquad \|\boldsymbol{J}\| = \sqrt{1/2\, J_{ij}\, J_{ij}}\,, \tag{6}$$

where I_{ij} is any deviatoric 'strain-like' tensor, and J_{ij} is any deviatoric 'stress-like' tensor. These are the norms of VON MISES (1913), where the coefficients under the radical signs scale the theory for shear.

In the theory of creep, $\|\dot{\boldsymbol{\varepsilon}}^p\|_{\text{ss}}$ is described by a kinetic equation, *i.e.* an equation of state. ZENER and HOLLOMON (1944) determined that such a kinetic equation can, to a good approximation, be decomposed into a product of two functions; in particular, at steady state

$$\|\dot{\boldsymbol{\varepsilon}}^p\|_{\text{ss}} = \vartheta[T]\, Z_{\text{ss}}\left[\frac{\|\boldsymbol{S}\|}{C}\right] \geq 0\,, \tag{7}$$

where $\vartheta > 0$ is a thermal function, $Z \geq 0$ is the Zener parameter, and $C > 0$ is a strength parameter that normalizes the stress. The Zener parameter is a temperature normalized measure of the plastic strain-rate. Square brackets, $[\cdot]$, are used throughout the paper to denote 'function of', and are therefore kept logically separate from parentheses, $(\cdot)$, which are used for mathematical groupings.

In the physical description of the thermal function, ϑ, there is a parameter called the activation energy, Q, which—for creep at low stresses and elevated temperatures—is associated with self-diffusion where the rate-controlling mechanism for deformation is dislocation climb (SHERBY and WEERTMAN, 1979). At higher stresses and/or more moderate temperatures, the rate-controlling mechanism changes from diffusion-controlled dislocation climb to obstacle-controlled dislocation glide (KOCKS *et al.*, 1975). Along with this change in the deformation mechanism, there occurs a change in the activation energy (SHERBY and BURKE, 1968). MILLER (1976) approximates the observed temperature dependence of the activation energy for steady-state flow with a linear function for temperatures below some threshold temperature, T_t, while for temperatures above this threshold the activation energy is kept constant, in accordance with the experimental observations of DORN (1954). Because it is the free energy (not the activation energy) that drives the kinetics of plastic deformation (KOCKS *et al.*, 1975), Miller integrated his linear function for the activation energy and obtains the following Arrhenius-like expression for the thermal function,

$$\vartheta = \begin{cases} \exp\left[\dfrac{-Q}{kT}\right] & \text{when} \quad T_t \leq T < T_m \\ \exp\left[\dfrac{-Q}{kT_t}\left(\ln\left[\dfrac{T_t}{T}\right] + 1\right)\right] & \text{when} \quad 0 < T \leq T_t \end{cases}, \tag{8}$$

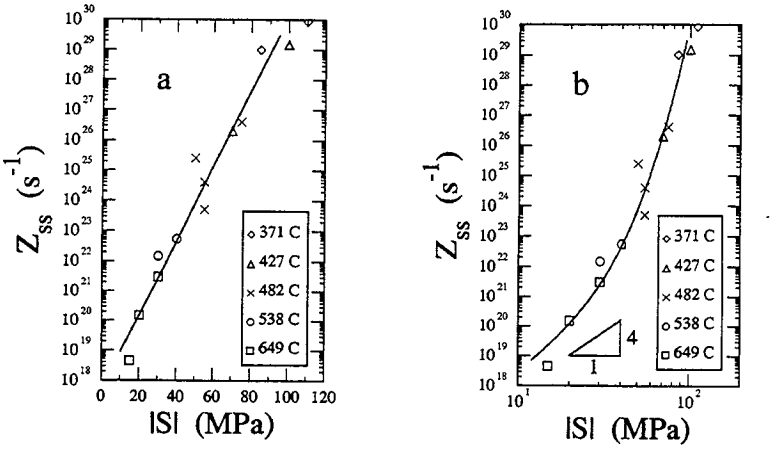

Figure 1: Steady-state creep behavior of NARloy Z. Data are from LEWIS (1970) with the reported material composition: Cu–2.89%Ag–0.22%Zr.

where k is the universal gas constant (8.314 J/mole-K). The applicability of this relationship is discussed elsewhere (FREED *et al.*, 1992). The transition temperature, T_t, between these two domains in activation energy is not unique; it is known to depend on the strain-rates used to make the measurements for activation energy. An increase in strain-rate increases the transition temperature (SHERBY and BURKE, 1968). For the vast majority of engineering applications, a transition temperature of $T_t \approx \frac{1}{2}T_m$ seems appropriate for f.c.c. metals, and is used in our characterization of NARloy Z.

When the mechanism for deformation changes from diffusion-controlled dislocation climb to obstacle-controlled dislocation glide, the creep response changes from power-law to exponential behavior (ASHBY, 1972). Following the approach of MILLER (1976), we adopt GAROFALO'S (1963) empirical expression for the steady-state Zener parameter, *i.e.*

$$Z_{ss} = A \sinh^n \left[\frac{\|S\|}{C} \right] , \tag{9}$$

where $A > 0$, $C > 0$ and $n > 0$ are the material constants. For stress states below power-law breakdown, *i.e.* when $\|S\| < C$, the steady-state Zener parameter of Garofalo reduces to the power-law relationship

$$Z_{ss} = A \left(\frac{\|S\|}{C} \right)^n , \tag{10}$$

thereby designating dislocation climb as the rate-controlling mechanism. (Note: A, C and n are independent in Eqn. (9) but not in Eqn. (10).) Similarly, when the stress exceeds power-law breakdown, *i.e.* when $\|S\| > C$, Garofalo's Zener parameter reduces to the exponential relationship

$$Z_{ss} = A' \exp \left[\frac{\|S\|}{C'} \right] , \tag{11}$$

where $A' = A/2^n$ and $C' = C/n$, thereby designating dislocation glide as the rate-controlling mechanism. The ability of Eqns (7–9) to correlate the stationary creep-rate data of NARloy Z is demonstrated in Fig. 1. The material constants obtained from this correlation are given in Table 2. Because none of these data lie within the power-law domain, the exponential creep equation, Eqn. (11), was used to determine values for A' and C' leading to the straight line fit shown in the log/linear plot of Fig. 1a, where $A' = 5 \times 10^{17}$ s^{-1} and $C' = 3.5$ MPa for the

Constant	Units	Value
A	s^{-1}	8×10^{18}
C	MPa	14
n	—	4
Q	J/mol.	450,000
T_m	K	~ 1350
$T_t = 1/2 T_m$		

Table 2: Steady-state creep constants for NARloy Z.

predefined values of $Q = 450,000$ J/mole (LEWIS, 1970) and $T_t = 400°C$ (assumed). Taking $n = 4$ (assumed), the values for A' and C' have been converted to those of A and C that are reported in Table 2. The result is the curved line presented in the log/log plot of Fig. 1b. We note that the value of C for NARloy Z, 14 MPa, obtained with this choice for n, 4, is in agreement with the value of C for Cu, 13 MPa, reported in FREED and WALKER (1993).

This continuum representation for creep is well established. Our viscoplastic model reduces analytically to this creep model under steady-state conditions. Hence, the material constants that characterize this creep model also appear in our viscoplastic model, which simplifies substantially its characterization process.

4 Viscoplastic Flow

A general mathematical structure for viscoplasticity (FREED *et al.*, 1991) may admit up to three kinds of internal state variables; they are: *i*) the (scalar-valued) drag strength, $D > 0$; *ii*) the (scalar-valued) yield stress, $Y \geq 0$; and *iii*) the (deviatoric tensor-valued) back stress, B_{ij}. The drag strength and yield stress account for isotropic hardening effects, while the back stress accounts for kinematic (flow-induced anisotropic) hardening effects.

PRAGER'S (1949) constitutive relation is used to describe the evolution of viscoplastic flow, *i.e.*

$$\dot{\varepsilon}^p_{ij} = 1/2 \, \|\dot{\boldsymbol{\varepsilon}}^p\| \, \frac{S_{ij} - B_{ij}}{\|\boldsymbol{S} - \boldsymbol{B}\|} \, . \tag{12}$$

This particular choice for the flow law implies that a nested set of flow surfaces exists; they are surfaces of constant plastic strain-rate when evaluated under isothermal conditions. This constitutes a set of ellipsoids in deviatoric stress space that are centered on the back stress.

The kinetics of viscoplasticity are taken to be described by a ZENER and HOLLOMON (1944) type decomposition of state (FREED *et al.*, 1991), *viz.*

$$\|\dot{\boldsymbol{\varepsilon}}^p\| = \vartheta[T] \, Z \left[\left\langle \frac{\|\boldsymbol{S} - \boldsymbol{B}\| - Y}{D} \right\rangle \right] \geq 0 \, , \tag{13}$$

where the Macauley bracket, $\langle (\|\boldsymbol{S} - \boldsymbol{B}\| - Y)/D \rangle$, has either a value of 0 whenever $\|\boldsymbol{S} - \boldsymbol{B}\| < Y$ (defining the elastic domain), or a value of $(\|\boldsymbol{S} - \boldsymbol{B}\| - Y)/D$ whenever $\|\boldsymbol{S} - \boldsymbol{B}\| > Y$ (defining the viscoplastic domain), with $\|\boldsymbol{S} - \boldsymbol{B}\| = Y$ establishing the yield surface. Many viscoplastic models have no distinct yield surface, *i.e.* they set Y to 0. The distinguishing feature between viscoplasticity (a rate-dependent theory) and plasticity (a rate-independent theory) is that viscoplasticity admits states both inside and outside of the yield surface (governed by a kinetic equation of state); whereas, plasticity admits only states that are inside and on the yield surface (governed by a consistency condition), but not outside of it. As a consequence, the plastic strain-rate is continuous as one moves from the elastic domain across the yield surface and into the inelastic domain of viscoplastic response; whereas, the accumulation of plastic strain is discontinuous as one moves from the elastic domain onto the yield surface in plasticity.

The elastic domain of many viscoplastic models is shrunk to a point, as they do not admit a yield surface.

The internal state variables—B_{ij}, D and Y—are described by evolution equations that are functions of state. The back stress evolves rapidly when compared with the rates of evolution for the drag strength and yield stress, which is a source of mathematical stiffness in the governing equations of viscoplasticity. The evolution of the back stress accounts for the change in material stiffness that is observed during the transition from elastic to plastic behavior, while the evolutions of the drag strength and yield stress account for the more gradual work hardening processes that are caused by the overall accumulation of plastic deformation. The internal variables are considered to evolve phenomenologically through competitive processes associated with strain hardening, strain-induced dynamic recovery, and time-induced thermal recovery. Their specific functional forms are discussed later in §6.

5 Creep $\Longleftrightarrow$ Viscoplasticity

In the process of going from creep theory to viscoplasticity, one must remove the steady-state constraint that is present in creep, and thereby extend the domain of admissible states to include transient behavior. This is done through the introduction of internal state variables. Although the purpose of viscoplasticity is to model rate-dependent transient behavior, it is not unreasonable to also require that it reduces to creep theory under steady-state conditions. An important objective in our development of a viscoplastic theory is that it reduces *analytically* to creep theory when at steady state. Not only is this a realistic requirement, but it also strengthens the physics of the theory, and it simplifies greatly the process of model characterization—about half of our viscoplastic material constants come from correlating stationary creep-rate data alone.

In order for a viscoplastic theory to reduce analytically to creep theory when at steady state (*i.e.* when $\dot{\boldsymbol{B}} = \boldsymbol{0}$, $\dot{D} = 0$ and $\dot{Y} = 0$ for $\|\dot{\boldsymbol{\varepsilon}}^p\| > 0$) two conditions must be satisfied. First, the back stress must be coaxial with the stress at steady state so that the directions of plastic strain-rate defined by Eqns (5 & 12) are also coaxial at steady state. And second, it is necessary that the kinetics of viscoplasticity, Eqn. (13), reduce analytically to the kinetics of creep, Eqn. (7), under steady-state conditions. Satisfaction of the first constraint is discussed in §6. To satisfy the second constraint, one must first hypothesize a relationship between the steady-state and transient Zener parameters, and then hypothesize another one between the internal and external variables, when at steady state (FREED and WALKER, 1990). We therefore suppose that

$$Z \equiv Z_{\rm ss}\left[\left\langle \frac{\|\boldsymbol{S}-\boldsymbol{B}\| - Y}{D} \right\rangle\right] , \tag{14}$$

in support of Eqn. (13). This relationship implies that the transient Zener parameter, Z, has the same functional form as the steady-state Zener parameter, $Z_{\rm ss}$, but with a different argument; in particular, and in accordance with Eqn. (9), we take

$$Z = A \sinh^n\left[\left\langle \frac{\|\boldsymbol{S}-\boldsymbol{B}\| - Y}{D} \right\rangle\right] , \tag{15}$$

which is similar in form to the kinetics of MILLER'S (1976) viscoplastic model, but with a yield stress and without a power acting on the Macauley bracket.

Furthermore, we shall suppose that

$$\|\boldsymbol{B}\|_{\rm ss} = f\,\iota_{\rm ss}[\|\boldsymbol{S}\|]\,\|\boldsymbol{S}\| \quad , \quad D_{\rm ss} = D_0 + \delta\,\|\boldsymbol{S}\| \quad \text{and} \quad Y_{\rm ss} = (1-f)\iota_{\rm ss}[\|\boldsymbol{S}\|]\,\|\boldsymbol{S}\| , \tag{16}$$

in support of experimental evidence, where $\iota_{\rm ss} > 0$ and $\delta > 0$ are the steady-state fractions of applied stress that are associated with the internal stress (*i.e.* the back and yield stresses) and the drag strength, respectively, such that $1/2 < \iota_{\rm ss} < 1$. The parameter f partitions the internal

stress between isotropic and kinematic contributions, such that $0 < f < 1$. The fact that drag strength is taken to be proportional to the saturation stress is a consequence of the fact that the drag strength represents the material's innate strength to resist plastic flow, *i.e.* D is a strength parameter—not a stress parameter. We take the internal stress to be a nonlinear function of the applied stress at saturation because that is what the experimental data of ARGON and TAKEUCHI (1981) and ČADEK (1987) suggest. A similar hypothesis to that of Eqn. (16) is given in FREED and WALKER (1993) for the case where the internal stress is composed of two back stresses with no yield stress.

Because the applied stress and the back stress must be coaxial at steady state, as discussed above, it follows that

$$\|\boldsymbol{S} - \boldsymbol{B}\|_{\rm ss} \;=\; \|\boldsymbol{S}\| - \|\boldsymbol{B}\|_{\rm ss} \,. \tag{17}$$

Therefore, upon equating the arguments of the Zener parameters in Eqns (7 & 14), while utilizing Eqns (16 & 17), one obtains the result

$$\iota_{\rm ss} = \frac{C - D_0 - \delta\,\|\boldsymbol{S}\|}{C} \;=\; \frac{C - D_0 + \sqrt{(C - D_0)^2 - 4\,\delta\,C\,(\|\boldsymbol{B}\|_{\rm ss} + Y_{\rm ss})}}{2\,C} \,. \tag{18}$$

If one uses Eqn. (16) and writes $\|\boldsymbol{B}\|_{\rm ss} + Y_{\rm ss} = \iota_{\rm ss}\,[\|\boldsymbol{S}\|]\;\|\boldsymbol{S}\|$, then from Eqn. (18) one determines that $\|\boldsymbol{B}\|_{\rm ss} + Y_{\rm ss} = (C - D_0 - \delta\|\boldsymbol{S}\|)\,\|\boldsymbol{S}\|/C$. Because $\partial\,(\|\boldsymbol{B}\|_{\rm ss} + Y_{\rm ss})\,/\partial\|\boldsymbol{S}\| = 0$ establishes the maximum state of internal stress, one is lead to the result

$$\|\boldsymbol{S}\|_{\rm max} = \frac{C - D_0}{2\,\delta} \,. \tag{19}$$

Substituting this relationship back into Eqns (16 & 18) gives additional upper bounds for: the back stress,

$$\|\boldsymbol{B}\|_{\rm max} = f\,\frac{(C - D_0)^2}{4\,\delta\,C} \,, \tag{20}$$

the drag strength,

$$D_{\rm max} = {}^1\!/_2\,\left(C + D_0\right) \,, \tag{21}$$

and the yield stress,

$$Y_{\rm max} = (1 - f)\frac{(C - D_0)^2}{4\,\delta\,C} \,. \tag{22}$$

Similar bounds are given in FREED and WALKER (1993) for the case where the internal stress is composed of two back stresses and no yield stress. *It is a remarkable fact that one can bound the stress and internal state variables without specifying anything about how these internal state variables evolve.*

Restricting $\iota_{\rm ss}$ to be real valued, and considering $\iota_{\rm min}$ to be associated with the maximum attainable magnitude of internal stress, one finds on approaching the limit of zero stress that the ratio of internal stress to applied stress at steady state is at its maximum, *i.e.*

$$\lim_{\|\boldsymbol{S}\|\to 0}\;\iota_{\rm ss} \equiv \iota_{\rm max} = \frac{C - D_0}{C} \approx 1 \,, \tag{23}$$

which is in reasonable agreement with ARGON and TAKEUCHI'S (1981) and ČADEK'S (1987) experimental observations. Approaching the limit of maximum stress, this ratio attains its minimum, *i.e.*

$$\lim_{\|\boldsymbol{S}\|\to\|\boldsymbol{S}\|_{\rm max}}\;\iota_{\rm ss} \equiv \iota_{\rm min} = \frac{C - D_0}{2\,C} \approx {}^1\!/_2 \,, \tag{24}$$

which is in reasonable agreement with LOWE and MILLER'S (1983) and ARGON and BHATTACHARYA'S (1987) experimental observations. A schematic of the steady-state internal stress versus the applied stress—as predicted by Eqns (16 & 18) with typical values of $D_0 = C/100$ and $f = 0.6$—is presented in Fig. 2. The trends depicted therein are in qualitative agreement

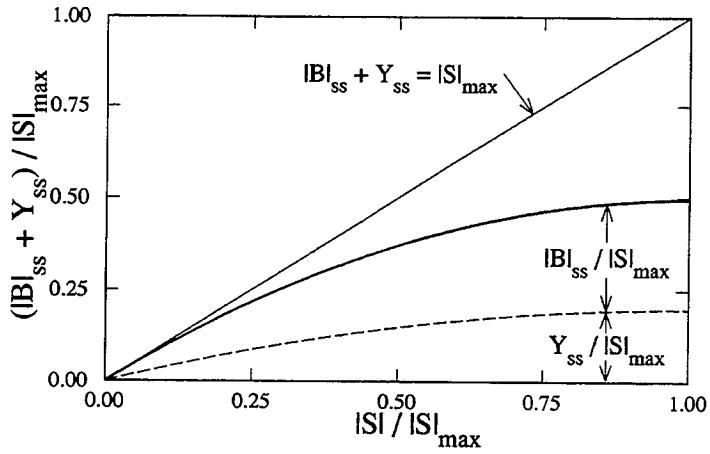

Figure 2: Schematic of internal stress (back plus yield stresses) at steady state *vs.* applied stress.

with the experimental results referenced above.

To be physically meaningful, $\|\boldsymbol{B}\| \geq 0$, $D > 0$ and $Y \geq 0$. Furthermore, their steady-state values ought to increase monotonically with increasing stress (FREED and WALKER, 1990). This is verified easily for our hypothesis, Eqns (14, 16 & 17), as long as $0 \leq \|\boldsymbol{B}\| \leq \|\boldsymbol{B}\|_{\max}$, $D_0 \leq D \leq D_{\max}$ and $0 \leq Y \leq Y_{\max}$.

6 Evolution of Internal State

The back stress is an internal stress caused by the heterogeneity of dislocation substructures (NIX and ILSCHNER, 1980) whose evolution is described adequately by the relationship of ARMSTRONG and FREDERICK (1966), *viz.*

$$\dot{B}_{ij} = 2H\left(\dot{\varepsilon}^p_{ij} - \frac{B_{ij}}{2L}\,\|\dot{\boldsymbol{\varepsilon}}^p\|\right) , \tag{25}$$

where $H[\xi] > 0$ is its hardening modulus, $L[D] \geq 0$ is its limiting state, and ξ is a normalized distance between the current position of the back stress in state space and its image point on the limit surface, as illustrated in Fig. 3. AIFANTIS (1986) derived this evolution equation for back stress from his single-slip dislocation theory. This nonlinear kinematic hardening rule, made popular by CHABOCHE (1977) with H and L as constants, is a three-dimensional representation of VOCE'S (1948) one-dimensional hardening rule. PRAGER'S (1949) linear kinematic hardening rule is the special case where H is a constant and $L = \infty$.

The back stress traverses a curve in stress space whose composition is a sequence of increments, dB_{ij}, wherein each increment lies along the instantaneous line segment joining the back stress with its current image point, as illustrated in Fig. 3. At kinematic saturation, *i.e.* when $\dot{\boldsymbol{B}} = \boldsymbol{0}$ for $\|\dot{\boldsymbol{\varepsilon}}^p\| > 0$, one can determine straight away from Eqns (12 & 25) that the plastic strain-rate, $\dot{\varepsilon}^p_{ij}$, becomes coaxial with both the deviatoric stress, S_{ij}, and the back stress, B_{ij}, in agreement with both experiment (PHILLIPS, 1986) and the hypothesis stated earlier in §5. Furthermore, the nested set of flow surfaces, $\{\|\boldsymbol{S}-\boldsymbol{B}\|-Y = \text{constant} \geq 0\}$, becomes stationary until unloading occurs; otherwise, the center of this set, B_{ij}, translates freely within its limiting hypersurface, L, as governed by the flow and evolution equations.

The limiting state of back stress, $L[D]$, is considered to depend on the drag strength (FREED and WALKER, 1993), thereby enabling the back stress to have an isotropic strengthening effect

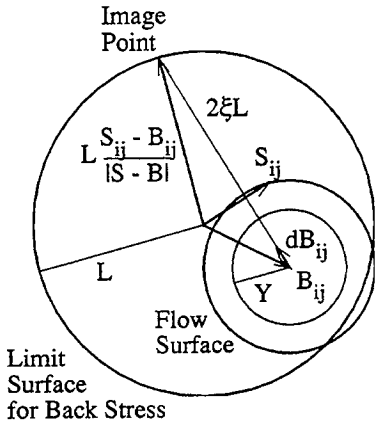

Figure 3: Evolution of back stress in state space representation.

(a concept introduced by MARQUIS, 1979). Because there is no explicit term for static recovery in the evolution equation for back stress, Eqn. (25), thermal recovery can only be introduced implicitly through a dependence of the limiting state on drag strength. This dependence, or coupling, enables our viscoplastic model to reduce analytically to creep theory under steady-state conditions. At kinematic saturation, $L_{ss}[D] = \|\boldsymbol{B}\|_{ss}$ which leads to the relationship

$$L = f\,\frac{(D - D_0)(C - D)}{\delta\, C}\,, \tag{26}$$

where use has been made of the hypothesis given in Eqn. (16). The subscripts 'ss' on D and $\iota[\|\boldsymbol{S}\|]$ in Eqn. (16) have been removed in the derivation of L because steady state is assumed to be only a special case. It follows that $0 \le \|\boldsymbol{B}\| \le \|\boldsymbol{B}\|_{\max}$ provided that $D_0 \le D \le D_{\max}$.

A measure of the distance between the back stress, B_{ij}, in stress space and its imaging point, $L(S_{ij} - B_{ij})/\|\boldsymbol{S} - \boldsymbol{B}\|$, on the limit (bounding) surface is characterized by

$$\xi = \sqrt{\frac{1}{8}\left(\frac{S_{ij}-B_{ij}}{\|\boldsymbol{S}-\boldsymbol{B}\|} - \frac{B_{ij}}{L}\right)\left(\frac{S_{ij}-B_{ij}}{\|\boldsymbol{S}-\boldsymbol{B}\|} - \frac{B_{ij}}{L}\right)}\,, \tag{27}$$

where $0 \le \xi \le 1$. This relationship comes from considering the state-space geometry shown in Fig. 3. The chord between the current state of back stress and its image point has length $2\xi L$. A value of $\xi = 0$ implies that B_{ij} is on its limit surface, and that S_{ij} is either on this surface or lies outside of it. A value of $\xi = 1$ also implies that B_{ij} is on its limit surface, but now S_{ij} lies inside this surface, *i.e.* unloading from a saturation state has just begun. The intermediate values of $0 < \xi < 1$ imply that B_{ij} is somewhere inside its limit surface. Physically, the parameter ξ simulates the back and forth motion of mobile dislocations. During directional deformation these mobile dislocations become immobilized by obstacles, as represented by $\xi \to 0$. Later, these immobilized dislocations may be released when the direction of loading is reversed, as represented by the switching action of ξ from $\xi \approx 0$ at the end of loading to $\xi \approx 1$ at the onset of unloading. This phenomenon is used to influence how we model the hardening and dynamic recovery behaviors of the internal state variables.

Prior experience in characterizing materials where Eqn. (25) describes the evolution of back stress has lead us to the rule-of-thumb: $H \approx \mu/5$. Unfortunately, this does not produce a smooth stress-strain transition between the elastic and plastic domains. This deficiency can be overcome by introducing multiple back stresses (CHABOCHE and ROUSSELIER, 1983, LOWE and

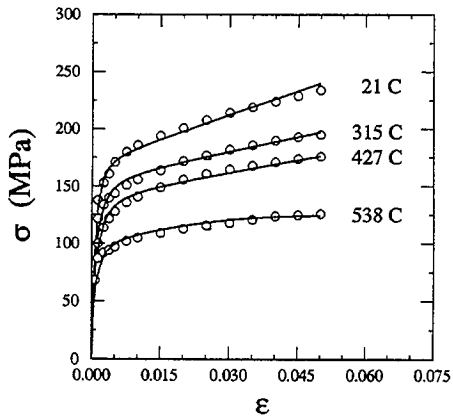

Figure 4: Tensile stress-strain curves for NARloy Z. Data are from the *Materials Properties Manual* (1986). Experiment (o) *vs.* theory (—). $\dot{\epsilon} = 0.001\ \mathrm{s}^{-1}$ (assumed), $D|_{t=0} = 2.02$ MPa (for $T = 21$ and 538°C) and $D|_{t=0} = 2.64$ MPa (for $T = 315$ and 427°C).

MILLER, 1986, and FREED and WALKER, 1993) with different hardening moduli or, as we have done herein, by making the hardening modulus a function of state. In particular, we have taken

$$H = (0.1 + 0.9\xi)\,\mu\,, \tag{28}$$

such that $\mu/10 \leq H \leq \mu$. This is similar in concept to the hardening modulus used by DAFALIAS and POPOV (1975) in their two-surface theory of plasticity, and by ROBINSON (1978) in his theory of viscoplasticity. The upper bound, $H = \mu$, produces a smooth stress-strain transition between the elastic and plastic responses. The lower bound, $H = \mu/10$, is set arbitrarily such that our rule-of-thumb value resides at the midpoint in the range of H. Setting the lower bound at a smaller value will lead to erroneous predictions; for example, when small stress-strain loops are contained within a larger hysteresis loop, the smaller loops will be too square in shape. There is no loss of generality by assuming the values 0.1 and 0.9 in Eqn. (28) because the partitioning parameter, f, between the isotropic and kinematic internal stresses is still at the modeler's disposal to adjust the shape of, say, stress-strain hysteresis loops.

The drag strength is considered to evolve as a competition between strain hardening and thermal (static) recovery phenomena, as expressed by

$$\dot{D} = h\,(\|\dot{\boldsymbol{\epsilon}}^p\| - \vartheta\, r)\ , \tag{29}$$

where $h > 0$ is its hardening modulus, $\vartheta[T] > 0$ is the thermal function of Eqn. (8), and $r[D] \geq 0$ is the thermal (static) recovery function. Herein, the hardening modulus, h, was taken to be a constant. This is sufficient for an adequate description of the tensile response shown in Fig. 4 for NARloy Z. In FREED and WALKER (1993), we have shown that taking h to be a function of state is equivalent to introducing a separate dynamic recovery term into the evolution equation for drag strength, Eqn. (29). Such a nonlinear hardening modulus for drag strength would cause greater curvatures in the predictions than those that are shown in Fig. 4.

At isotropic saturation, *i.e.* when $\dot{D} = 0$ for $\|\dot{\boldsymbol{\epsilon}}^p\| > 0$, one readily determines from Eqn. (29) that $r_{ss} = Z_{ss}$. Upon substituting Eqn. (16) into Eqn. (9), one therefore obtains

$$r = A\,\sinh^n\!\left[\frac{D - D_0}{\delta\, C}\right]\ , \tag{30}$$

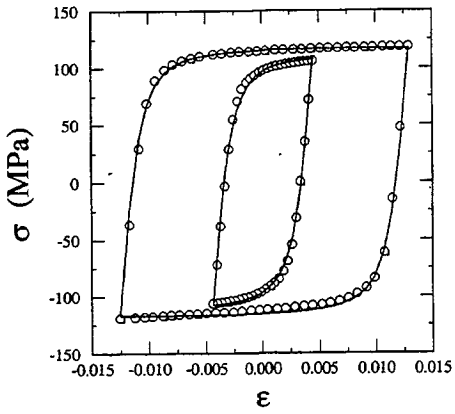

Figure 5: Saturated hysteresis loops for NARloy Z. Data are from CONWAY *et al.* (1975). Experiment (o) *vs.* theory (—). $\dot{\epsilon} = 0.004\ \mathrm{s}^{-1}$, $T = 538°\mathrm{C}$, $D|_{\Delta\epsilon=0.009} = 2.19$ MPa and $D|_{\Delta\epsilon=0.026} = 2.32$ MPa.

which describes all thermal recovery behavior in our model. Recall that there is no explicit thermal recovery of the back stress. Again, the subscript 'ss' is deleted from D implying that transient states are not given special treatment.

Although the effect of a separate, dynamic, recovery term in the evolution equation for drag strength is not deemed to be important in the monotonic description of NARloy Z (see Fig. 4), there is an effect similar to that which is very important, *viz.* the interaction between monotonic and cyclic plasticity. This effect is illustrated in Fig. 5 where saturated, stress-strain, hysteresis loops are presented for NARloy Z. If one were to use Eqn. (29) to describe the evolution of drag strength, then the two hysteresis loops in Fig. 5 would be predicted to have the same stress range even though their strain ranges differ significantly. Certainly this does not agree with the experimental results shown, nor is it in agreement with typical metallic behavior (LANDGRAF *et al.*, 1969). To accommodate this behavior, a dynamic recovery term is introduced into Eqn. (29) such that

$$\dot{D} = h\Big(\|\dot{e}^p\| - \Lambda\,\|\dot{e}^p\| - \vartheta\, r\Big)\ , \tag{31}$$

where $\Lambda[\xi] \geq 0$ is the monotonic/cyclic interaction term with $\Lambda_{ss} = 0$. This evolution law is similar in form and motivation to the one used by MILLER (1976) in his viscoplastic model. What distinguishes this dynamic recovery term from others found in the literature is that ours depends on ξ instead of $D - D_0$. In order to be compatible with the derivation of r given above, Λ_{ss} must be 0. The material function ξ, which is a measure of the back and forth (directional) motion of mobile dislocations, is the physically based parameter that we use to describe the monotonic/cyclic interaction effect. It is a much simpler concept to utilize, especially under non-isothermal conditions, than the idea of a strain memory surface introduced by CHABOCHE *et al.* (1979).

The monotonic/cyclic interaction function is taken to be described by a simple linear relationship, *viz.*

$$\Lambda = \ell\,\xi\ , \tag{32}$$

where $\ell > 1$ is a material constant. This has the desired property that $\Lambda_{ss} = 0$ because $\xi_{ss} = 0$. Also, since ξ is bound by 0 and 1, Λ is bound by 0 and ℓ. If there is to be any interaction effect

at all, ℓ must be greater than 1 so that the quantity $\|\dot{\varepsilon}^p\| - \Lambda \|\dot{\varepsilon}^p\|$ may become negative valued during unloading.

Because the drag strength and yield stress are both isotropic internal variables, they most likely both evolve due to the same physical mechanism—a variation in the dislocation density. Consequently, only one of these two internal variables, the drag strength, is taken to be an independent variable. We therefore assume that the yield stress can be described as a state function of drag strength, *i.e.* $Y[D]$, which helps keep our viscoplastic model simple. Taking the expression for $Y_{\rm ss}[\|\boldsymbol{S}\|]$ given in Eqn. (16), combining it with Eqn. (18), and then using the expression for $\|\boldsymbol{S}\|[D_{\rm ss}]$ also given in Eqn. (16), one obtains

$$Y = (1-f)\frac{(D-D_0)(C-D)}{\delta\, C}\,, \tag{33}$$

where the subscript 'ss' has been removed, implying that transient states are not given special treatment.

7 The Model

Here we combine the results of the previous sections to give a succinct description of our viscoplastic model. The stress is acquired through the constitutive equations

$$S_{ij} = 2\mu\Big(E_{ij} - \varepsilon^p_{ij}\Big) \qquad \text{and} \qquad \sigma_{kk} = 3\kappa\Big(\epsilon_{kk} - \alpha(T-T_0)\delta_{kk}\Big)\,. \tag{34}$$

The flow equation and kinetics that describe plastic straining are given by

$$\dot{\varepsilon}^p_{ij} = {}^1\!/_2\,\|\dot{\varepsilon}^p\|\,\frac{S_{ij}-B_{ij}}{\|\boldsymbol{S}-\boldsymbol{B}\|} \qquad \text{and} \qquad \|\dot{\varepsilon}^p\| = \vartheta\, Z\,, \tag{35}$$

respectively, with the von Mises norm of effective stress being defined by

$$\|\boldsymbol{S}-\boldsymbol{B}\| = \sqrt{{}^1\!/_2\,(S_{ij}-B_{ij})\,(S_{ij}-B_{ij})}\,. \tag{36}$$

The evolutions of back stress and drag strength are given by

$$\dot{B}_{ij} = 2H\left(\dot{\varepsilon}^p_{ij} - \frac{B_{ij}}{2\,L}\,\|\dot{\varepsilon}^p\|\right) \qquad \text{and} \qquad \dot{D} = h\Big(\|\dot{\varepsilon}^p\| - \Lambda\,\|\dot{\varepsilon}^p\| - \vartheta\, r\Big)\,, \tag{37}$$

respectively, such that $D_0 \le D \le D_{\rm max}$, while the yield stress is related through the state function

$$Y = (1-f)\frac{(D-D_0)(C-D)}{\delta\, C}\,, \tag{38}$$

which is not an evolution equation. Associated with these relationships are the material functions:

$$\vartheta = \begin{cases} \exp\left[\dfrac{-Q}{kT}\right] & \text{when} \quad T_t \le T < T_m \\[2ex] \exp\left[\dfrac{-Q}{kT_t}\left(\ln\left[\dfrac{T_t}{T}\right] + 1\right)\right] & \text{when} \quad 0 < T \le T_t \end{cases}\,, \tag{39}$$

$$Z = A\,\sinh^n\left[\left\langle\frac{\|\boldsymbol{S}-\boldsymbol{B}\| - Y}{D}\right\rangle\right]\,, \tag{40}$$

$$H = (0.1 + 0.9\,\xi)\,\mu \qquad \text{and} \qquad L = f\,\frac{(D-D_0)(C-D)}{\delta\, C}\,, \tag{41}$$

$$\Lambda = \ell\,\xi \qquad \text{and} \qquad r = A\,\sinh^n\left[\frac{D-D_0}{\delta\, C}\right]\,, \tag{42}$$

with

$$\xi = \sqrt{\frac{1}{8}\left(\frac{S_{ij}-B_{ij}}{\|\boldsymbol{S}-\boldsymbol{B}\|} - \frac{B_{ij}}{L}\right)\left(\frac{S_{ij}-B_{ij}}{\|\boldsymbol{S}-\boldsymbol{B}\|} - \frac{B_{ij}}{L}\right)} \,. \tag{43}$$

Restricting the drag strength to be bound by the interval $D_0 \leq D \leq D_{\max}$ restricts automatically the remaining variables: $0 \leq \|\boldsymbol{S}\| \leq \|\boldsymbol{S}\|_{\max}$, $0 \leq \|\boldsymbol{B}\| \leq \|\boldsymbol{B}\|_{\max}$ and $0 \leq Y \leq Y_{\max}$.

For uniaxial loading histories in tension and compression, the above governing equations hold with the following alterations:

$$\sigma = E\left(\epsilon - \varepsilon^p - \alpha(T-T_0)\right) \quad , \quad \dot{\varepsilon}^p = \operatorname{sgn}[\sigma-\beta]\,\frac{\|\dot{\boldsymbol{\varepsilon}}^p\|}{\sqrt{3}} \quad \text{and} \quad \dot{\beta} = 3\,H\left(\dot{\varepsilon}^p - \frac{\beta}{3\,L}\,\|\dot{\boldsymbol{\varepsilon}}^p\|\right) \,, \tag{44}$$

given that $\sigma = \sigma_{11} = {}^3\!/_2\, S_{11}$, $\beta = \beta_{11} = {}^3\!/_2\, B_{11}$, $\epsilon = \epsilon_{11}$ and $\varepsilon^p = \varepsilon^p_{11}$. As for the material functions, the above equations apply with the following alterations:

$$Z = A\,\sinh^n\left[\left\langle\frac{|\sigma-\beta| - \sqrt{3}\,Y}{\sqrt{3}D}\right\rangle\right] \qquad \text{and} \qquad \xi = {}^1\!/_2\left|\operatorname{sgn}[\sigma-\beta]1 - \frac{\beta}{\sqrt{3}L}\right| \,. \tag{45}$$

This one-dimensional model has been applied to NARloy Z in this paper.

8 Characterization

Of the eleven, temperature independent, material constants required to characterize this viscoplastic model, *viz.* the set $\{A,\ C,\ \delta,\ D_0,\ f,\ h,\ \ell,\ n,\ Q,\ T_m,\ T_t\}$, the melting temperature, T_m, and the activation energy for self-diffusion, Q, are physical properties that can usually be found in the literature (*e.g.* SHERBY and WEERTMAN, 1979). If Q is not available, it can be determined readily from creep experiments (see DORN, 1954, or SHERBY and BURKE, 1968) at temperatures in excess of about ${}^1\!/_2\, T_m$. Herein, we have set $T_t = {}^1\!/_2\, T_m$, and we have taken Q from the literature (LEWIS, 1970). Because T_m[NARloy Z] $< T_m$[Cu] = 1356 K, we took T_m = 1350 K (its actual value is unknown to us). Thus, the temperature dependence of the model is established first.

With the thermal function, ϑ, now characterized by Eqn. (8), one can determine the steady-state Zener parameter, $Z_{\text{ss}} = \|\dot{\boldsymbol{\varepsilon}}^p\|_{\text{ss}}/\vartheta$, from creep data and plot it against its associated flow stress, $\|\boldsymbol{S}\|$, as done in Fig. 1 using the norms defined in Eqn. (6). The curve in Fig. 1b represents a fit of GAROFALO'S (1963) creep equation, Eqn. (9), to the data. From this fitting procedure, one obtains the constants A, C and n reported in Table 2. This completes the strain-rate sensitivity characterization of the model; it is the characterization of creep described in §3.

The next step in the characterization process is to establish the maximum values that can be attained by the stress and the internal variables via a determination for the value of δ. One way to establish its value is to take the ultimate tensile strength at a very low temperature—*e.g.* from the literature (*Materials Properties Manual*, 1986) we found σ_{ult} = 325 MPa, or equivalently $\|\boldsymbol{S}\|_{\text{ult}}$ = 190 MPa, at −82 °C for NARloy Z—and define this value to be the maximum attainable stress, *viz.* $\|\boldsymbol{S}\|_{\max}$ = 190 MPa for NARloy Z. From Eqn.(19), recall that $\|\boldsymbol{S}\|_{\max} = (C - D_0)/2\delta \approx C/2\delta$ (because $D_0 \ll C$, typically). Since we already know the value for C (it is 14 MPa for NARloy Z) from our characterization of creep behavior, one determines quickly the value for δ (it is 0.035 for NARloy Z, which is the same value obtained for Cu by FREED and WALKER, 1993). This derivation requires D_0 to be small with respect to C. FREED and WALKER (1993) found $D_0 \approx C/100$ for f.c.c. metals, and this value is assumed here for NARloy Z. If data are available, which they are not for NARloy Z, one may obtain the value for D_0 by correlating an experimental, offset, yield stress with the model's prediction. This requires a specimen in its softest possible (annealed) state; in such a state, NARloy Z would resemble Cu.

The partitioning of the internal stress between isotropic and kinematic contributions via f is the next step in the process of parameter estimation. Saturated, stress-strain, hysteresis loops

Constants	Units	Value
δ	—	0.035
f	—	0.65
h	MPa	11
ℓ	—	6.4
$D_0 = C/100$		

Table 3: Additional viscoplastic constants for NARloy Z.

are suited ideally for this purpose, because in this case the drag strength can be treated as a material constant. Although it is not necessary, we have found it to be expedient to utilize the Levenberg-Marquardt minimization method (outlined in the Appendix) to determine an optimal value for the material constant f (along with D). The outcome is shown in Fig. 5. Even though f is bound by the interval (0, 1), the partitioning between isotropic and kinematic contributions in the internal stress, f, is more realistically bound by the interval (0.25, 0.75). Its actual value is given in Table 3. This completes the characterization for the evolution of back stress.

All that remains for us to quantify is how the drag strength evolves. This is done in two steps. First, one must ascertain a value for the hardening modulus, h, and second, one must determine the strength of the monotonic/cyclic interaction effect via ℓ. Values for these material constants are also given in Table 3.

The hardening modulus h establishes the rate of isotropic hardening. Its value is best acquired from stress-strain curves of annealed material, where the back stress is basically saturated (*i.e.* on its limit surface) throughout the test. Consequently, there is negligible influence due to the monotonic/cyclic interaction term since $\Lambda \approx 0$ throughout the test, and therefore the dynamic recovery term, $\Lambda \|\dot{\epsilon}^p\|$, can be omitted from the drag strength's evolution law during this step. Figure 4 presents the model's correlations obtained at this stage of the parameter estimation process. Once again we have used the Levenberg-Marquardt minimization method to determine an optimal value for h (along with $D|_{t=0}$). There are two distinct values for $D|_{t=0}$ reported in Fig. 4, which suggests that these tests may have come from two different batches of material, but this is only conjecture.

The final step in the process of characterizing a material is the quantification of the monotonic/cyclic interaction effect. To accomplish this we reconsider the saturated hysteresis loops given in Fig. 5, but now the drag strength is allowed to evolve. By adjusting the value of ℓ, which was done easily through trial and error, the stress range for the loop $\epsilon = \pm 0.0045$ in Fig. 6 was fit, while the remaining loops are given as theoretical predictions. The loops for $\epsilon = \pm 0.0025$ and ± 0.0075 have no experimental data for comparison. The larger the value for ℓ, the greater the curvature in the cyclic stress-strain curve, which can be described by connecting the tips of the fully-reversed, stress-strain, hysteresis loops of differing strain ranges.

9 Closure

By designing the development of our viscoplastic model in such a manner that it reduces analytically to a creep model under steady-state conditions, we have incorporated some essential physics into our model, and we have also simplified greatly the process that one must go through in order to characterize a material with this model. In this sense, we have developed a viscoplastic model with an eye towards its characterization. This has particular merit because parameter estimation of a viscoplastic model is, in general, a complex process that very often prohibits its use in applications. A model's ease of characterization without the need of exotic experiments is often considered by many industrial users of viscoplasticity to be of greater value than the model's ability to predict accurately a material's behavior (within reason). Our model was de-

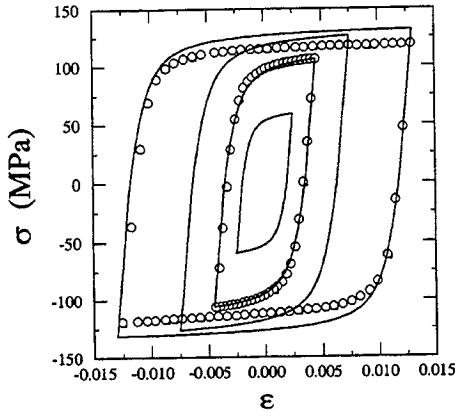

Figure 6: Saturated hysteresis loops for NARloy Z. Data are from CONWAY *et al.* (1975). Experiment (o) *vs.* theory (—). $\dot{\epsilon} = 0.004\,\mathrm{s}^{-1}$ and $T = 538°\mathrm{C}$.

veloped with this fact in mind, where we have sought to strike a balance between accuracy and ease of characterization using physics as our guidepost.

Acknowledgment

The work of one of the authors (KPW) was supported by the United States Department of Energy under Grant Number DE–FG02–92ER14247. Dr. Oscar P. Manley served as contract monitor.

References

——, 1986, *Materials Properties Manual*, Vol. III, 4th ed., Rockwell International, Rocketdyne Division, Canoga Park, CA.

AIFANTIS, E.C., 1986, "On the Structure of Single Slip and its Implications for Inelasticity," in GITTUS, J. *et al.* (eds.), *Large Deformations of Solids*, Elsevier, Amsterdam, pp. 283–325.

ARGON, A.S. and BHATTACHARYA, A.K., 1987, "Primary Creep in Nickel: Experiments and Theory," *Acta Metall.*, Vol. 35, pp. 1499–1514.

ARGON, A.S. and TAKEUCHI, S., 1981, "Internal Stresses in Power-Law Creep," *Acta Metall.*, Vol. 29, pp. 1877–1884.

ARMSTRONG, P.J. and FREDERICK, C.O., 1966, "A Mathematical Representation of the Multiaxial Bauschinger Effect," Central Electric Generating Board, Berkeley Nuclear Laboratories, Report RD/B/N731.

ASHBY, M.F., 1972, "A First Report on Deformation-Mechanism Maps," *Acta Metall.*, Vol. 20, pp. 887–897.

ČADEK, J., 1987, "The Back Stress Concept in Power Law Creep of Metals: A Review," *Mater. Sci. Engrg.*, Vol. 94, pp. 79–92.

CHABOCHE, J.-L., 1977, "Viscoplastic Constitutive Equations for the Description of Cyclic and Anisotropic Behavior of Metals," *Bull. Acad. Pol. Sci., Ser. Sci. Tech.*, Vol. 25, pp. 39–48.

CHABOCHE, J.-L., DANG-VAN, K. and CORDIER, G., 1979, "Modelization of the Strain Memory Effect on the Cyclic Hardening of 316 Stainless Steel," (ONERA TP 1979–109) in *SMIRT-5*, Div. L, August 13–21, Berlin.

CHABOCHE, J.-L. and ROUSSELIER, G., 1983, "On the Plastic and Viscoplastic Constitutive Equations," *J. Pres. Vessel Technol.*, Vol. 105, pp. 153–158.

CONWAY, J.B., STENTZ, R.H. and BERLING, J.T., 1975, "High-Temperature, Low-Cycle Fatigue of Copper-Base Alloys for Rocket Nozzles; Part I – Data Summary for Materials Tested in Prior Programs," NASA CR–134908, November.

DAFALIAS, Y.F. and POPOV, E.P., 1975, "A Model of Nonlinearly Hardening Materials for Complex Loading," *Acta Mech.*, Vol. 21, pp. 173–192.

DORN, J.E., 1954, "Some Fundamental Experiments on High Temperature Creep," *J. Mech. Phys. Solids*, Vol. 3, pp. 85–116.

FREED, A.D., CHABOCHE, J.-L. and WALKER, K.P., 1991, "A Viscoplastic Theory with Thermodynamic Considerations," *Acta Mech.*, Vol. 90, pp. 155–174.

FREED, A.D., RAJ, S.V. and WALKER, K.P., 1992, "Stress Versus Temperature Dependence of Activation Energies for Creep," *J. Engrg. Mater. Technol.*, Vol. 114, pp. 46–50.

FREED, A.D. and WALKER, K.P., 1990, "Steady-State and Transient Zener Parameters in Viscoplasticity: Drag Strength versus Yield Strength," (NASA TM–102487) *Appl. Mech. Rev.*, Vol. 43, No. 5, Pt. 2, pp. S328–S337.

FREED, A.D. and WALKER, K.P., 1993, "Viscoplasticity With Creep and Plasticity Bounds," in press: *Int. J. Plast.*, Vol. 9.

GAROFALO, F., 1963, "An Empirical Relation Defining the Stress Dependence of Minimum Creep Rate in Metals," *Trans. AIME*, Vol. 227, pp. 351–356.

KOCKS, U.F., ARGON, A.S. and ASHBY, M.F., 1975, "Thermodynamics and Kinetics of Slip," in CHALMERS, B. *et al.* (eds.), *Progress in Materials Science,* Pergamon Press, Oxford, Vol. 19.

LANDGRAF, R.W., MORROW, J. and ENDO, T., 1969, "Determination of the Cyclic Stress-Strain Curve," *J. Mater.*, Vol. 4, pp. 176–188.

LEWIS, J.R., 1970, "Creep Behavior of NARloy Z," Rockwell International, Rocketdyne Division, Canoga Park, CA, Report MA-SSE-70-902, July.

LOWE, T.C. and MILLER, A.K., 1983, "The Nature of Directional Strain Softening," *Scripta Metall.*, Vol. 17, pp. 1177–1182.

LOWE, T.C. and MILLER, A.K., 1986, "Modeling Internal Stresses in the Nonelastic Deformation of Metals," *J. Engrg. Mater. Technol.*, Vol. 108, pp. 365–373.

MARQUIS, D., 1979, "Modélisation et Identification de L'écrouissage Anisotrope des Métaux," Thèse de 3$^{\text{ème}}$ cycle, Université Paris VI.

MILLER, A., 1976, "An Inelastic Constitutive Model for Monotonic, Cyclic, and Creep Deformation," *J. Engrg. Mater. Technol.*, Vol. 98, pp. 97–105.

VON MISES, R., 1913, "Mechanik der festen Körper im plastisch-deformablen Zustand," *Nachr. Ges. Wiss., Goettingen, Math. Phys. Kl.*, pp. 582–592.

NIX, W.D. and ILSCHNER, B., 1980, "Mechanisms Controlling Creep of Single Phase Metals and Alloys," in HAASEN, P. *et al.* (eds.), *Strength of Metals and Alloys*, Pergamon Press, Oxford, pp. 1503–1530.

ODQVIST, F.K.G., 1974, *Mathematical Theory of Creep and Creep Rupture*, 2$^{\text{nd}}$ ed., Oxford University Press, London.

PHILLIPS, A., 1986, "A Review of Quasistatic Experimental Plasticity and Viscoplasticity," *Int. J. Plast.*, Vol. 2, pp. 315–328.

PRAGER, W., 1949, "Recent Developments in the Mathematical Theory of Plasticity," *J. Appl. Phys.*, Vol. 20, pp. 235–241.

ROBINSON, D.N., 1978, "A Unified Creep-Plasticity Model for Structural Metals at High Temperature," ORNL TM–5969.

SHERBY, O.D. and BURKE, P.M., 1968, "Mechanical Behavior of Crystalline Solids at Elevated Temperature," in CHALMERS, B. and HUME-ROTHERY, W. (eds.), *Progress in Materials*

Science, Pergamon Press, Oxford, Vol. 13, pp. 325–390.

SHERBY, O.D. and WEERTMAN, J., 1979, "Diffusion-Controlled Dislocation Creep: A Defense," *Acta Metall.,* Vol. 27, pp. 387–400.

VOCE, E., 1948, "The Relationship Between Stress and Strain for Homogeneous Deformation," *J. Inst. Metals,* Vol. 74, pp. 537–562.

ZENER, C. and HOLLOMON, J.H., 1944, "Effect of Strain Rate Upon Plastic Flow of Steel," *J. Appl. Phys.,* Vol. 15, pp. 22–32.

Appendix

The determination of the material constants in a viscoplastic model poses many difficulties, and it is facilitated greatly by using the modified, nonlinear, least-squares method of Levenberg and Marquardt (PILVIN, 1988). If x_n denotes the vector that contains the material constants to be determined, then the computed stress will depend on the material vector x_n and can be written as $\sigma\,[x_n]$, where n ranges from 1 to N, with N being the number of unknown material constants in the vector x_n. The test result corresponding to the computed value of $\sigma\,[x_n]$ is denoted by σ^T. To simplify the discussion, we consider strain, ϵ, to be the controlled parameter and stress, σ, to be the response parameter. This algorithm may also be applied to the inverse situation.

The material constant vector, x_n, can be determined by minimizing the square of the differences between the test results and the computed results at the user selected points 1, 2, ..., M belonging to a set of experimental data files. The total number of points in these data files will usually be much larger than M.

In the minimization procedure, the function to be minimized is

$$U[x_n] = \frac{1}{M}\sum_{r=1}^{M}\left(\sigma_r[x_n] - \sigma_r^T\right)^2 . \qquad (A1)$$

If x_n^G denotes an estimated, or guessed, value for the material constant vector, this vector will not result, in general, in a minimum value for the objective function U. Let the vector that does result in a minimum value be denoted by x_n. Then we can write

$$x_n = x_n^G + \Delta x_n \,, \qquad (A2)$$

where Δx_n is the amount, or correction, that must be added to the guessed value to produce the value which minimizes U. If the guessed vector, x_n^G, is close to the true vector, x_n, then the correction vector, Δx_n, will be small in comparison with x_n^G. By expanding the objective function into a Taylor series, the correction vector can be determined by solving the linear system of equations

$$\sum_{q=1}^{N} A_{pq}\Delta x_q = b_p \qquad \text{for} \qquad p = 1, 2, \ldots, N \,, \qquad (A3)$$

where

$$A_{pq} = \sum_{r=1}^{M}\left(\frac{\partial\sigma_r[x_n^G]}{\partial x_p}\right)\left(\frac{\partial\sigma_r[x_n^G]}{\partial x_q}\right) \qquad \text{and} \qquad b_p = -\sum_{r=1}^{M}\left(\sigma_r[x_n^G] - \sigma_r^T\right)\frac{\partial\sigma_r[x_n^G]}{\partial x_p} . \qquad (A4)$$

Because only the first term in the Taylor series is kept in the preceding expansion, the solution vector, Δx_n, is not exact; hence, iterative improvements must be made. This is the method of nonlinear least squares (also called the Hessian method). In application, the derivatives in Eqn. (A4) are found numerically.

Marquardt put forth an elegant algorithm, related to an earlier suggestion of Levenberg, for varying smoothly between the extremes of the methods of nonlinear least squares and steepest

descent (PRESS *et al.*, 1989). The Levenberg-Marquardt method accomplishes this by altering the A_{pq} matrix in Eqn. (A4) according to

$$A'_{pp} = (1+\lambda)A_{pp} \qquad \text{and} \qquad A'_{pq} = A_{pq} \quad \text{when} \quad p \neq q\,, \tag{A5}$$

and then replacing Eqn. (A3) with

$$\sum_{q=1}^{N} A'_{pq}\Delta x_q = b_p \qquad \text{for} \qquad p = 1, 2, \ldots, N\,. \tag{A6}$$

When λ is large, the matrix A'_{pq} becomes diagonally dominant and the algorithm approaches that of steepest descent; whereas, when λ is small, the matrix $A'_{pq} \simeq A_{pq}$ and the algorithm approaches that of nonlinear least squares.

The Marquardt-Levenberg method can still produce unacceptably large changes, Δx_q, in the material constant vector, x_q, if the trial vector is far from its final least squares value. An acceptable solution procedure which provides a stable approach to the least squares solution can be obtained by introducing a cutback parameter, ϵ, into the algorithm (WALKER and JORDAN, 1987). The user can then specify that the maximum percentage change, R, in any material constant is not to exceed an input value of c percent.

The modified numerical recipe then goes as follows:

1. Pick a maximum percentage change in any material constant, say $c = 20$.
2. Pick an initial value for λ, say $\lambda = 10$.
3. Compute $U[x_n^G]$.
4. Solve Eqn. (A6) for Δx_n.
5. Compute $R = \max_{q=1}^{N}\left(100 \times \frac{\Delta x_q}{x_q}\right)$.
6. If $R \leq c$, set cutback parameter $\epsilon = 1$.
7. If $R > c$, set cutback parameter $\epsilon = c/R$.
8. If $U[x_n^G + \epsilon\Delta x_n] \geq U[x_n^G]$, *increase* λ by a factor of 10 and return to step 4.
9. If $U[x_n^G + \epsilon\Delta x_n] < U[x_n^G]$, *decrease* λ by a factor of 10 and update $x_n^G \leftarrow x_n^G + \epsilon\Delta x_n$.
10. Exit if converged, else go back to step 4.

The Levenberg-Marquardt-cutback modifies the solution vector, Δx_q quite dramatically during the least squares solution procedure. For example, when the initial guess for the material constant vector, x_n^G, in the viscoplastic constitutive equations is far from the optimum least squares value, the nonlinearity can be large enough to cause the cutback parameter, ϵ, to be as small as 10^{-10}. That is, an element of the material constant vector, x_n^G, can change by up to 20% when the change, Δx_n, in that element is only 10^{-10} of that predicted by the Levenberg-Marquardt procedure. As the solution approaches its optimum least squares value, the parameter $\epsilon \rightarrow 1$ and the change in the material constants is governed by the full least squares value.

Appendix References

PILVIN, P., 1988, "Identification des Paramètres de Modèles de Comportement," in CAILLETAUD, G. *et al.* (eds.), *The Inelastic Behaviour of Solids: Models and Utilization,* Proceedings of MECAMAT, August 30 – September 1, Besançon, France, pp. 155–164.

PRESS, W.H., FLANNERY, B.P., TEUKOLSKY, S.A. and VETTERLING, W.T., 1989, *Numerical Recipes in Pascal*, Cambridge University Press, Cambridge.

WALKER, K.P. and JORDAN, E.H., 1987, "Constitutive Modelling of Single Crystal and Directionally Solidified Superalloys," in *Turbine Engine Hot Section Technology 1987*, NASA CP 2493, pp. 299–301.